Articular Cartilage Defects: Detectability in Cadaver Knees with MR

Victoria M. Gylys-Morin[1]
Paul C. Hajek
David J. Sartoris
Donald Resnick

The capability of 1.5-T MR imaging to detect focal defects in articular cartilage was investigated with cadaveric knees with and without intraarticular injection of saline and gadolinium-DTPA (Gd-DTPA). Full-thickness cartilage lesions ranging in diameter from 1 to 5 mm were surgically created in the femoral articular surfaces. Images were acquired with a variety of pulse techniques, slice thicknesses, and interslice gaps as well as one or two signal excitations. Potential intraarticular contrast agents (saline and Gd-DTPA) were tested, and their signal behaviors compared with that of hyaline cartilage. All cartilage defects were occult on T1-weighted and balanced images without Gd-DTPA. The smallest defect identified by using intraarticular saline was 3 mm in diameter and was apparent only on T2-weighted images. Intraarticular Gd-DTPA afforded detection of defects as small as 2 mm, even with short imaging times. Signal-intensity differences between saline and articular cartilage were minimal on T1-weighted images and increased on T2-weighted images; intensity differences were high between Gd-DTPA and articular cartilage on all imaging sequences.

These results indicate that intraarticular fluid and appropriate selection of imaging sequences are necessary for delineation of focal defects in articular cartilage. They also show that Gd-DTPA is the optimal contrast agent for this purpose.

MR imaging has been useful in depicting the normal anatomy of the knee joint as well as abnormalities involving the ligaments, menisci, and periarticular soft tissues [1–10]. Diagnostic imaging of articular cartilage constitutes an important aspect of the clinical evaluation of joint dysfunction. Contrast arthrography, computed arthrotomography, and arthroscopy have been used in the diagnosis of cartilage defects [6, 8, 11]. MR imaging, with its advantages of noninvasiveness, superior tissue contrast discrimination, adequate spatial resolution with surface-coil techniques, and ability to provide information about both intra- and extraarticular soft-tissue structures, is a promising new diagnostic method for evaluating articular cartilage defects in traumatic, degenerative, and inflammatory joint diseases.

On high-resolution surface-coil MR images, articular cartilage appears as two apposing layers of intermediate signal intensity adjacent to the dark signal of subchondral bone, measuring about 2 mm in thickness at weight-bearing sites [1, 9, 12]. While MR has been shown to be capable of delineating diffuse cartilage loss, its sensitivity in the detection of discrete cartilage defects has not been defined. To date, MR has proven to be successful in identifying only gross cartilage defects [1–3, 9].

To determine the lower limits of MR spatial resolution in detecting cartilage lesions, surgical defects were introduced in the articular cartilage of cadaveric knees. Optimal imaging parameters were determined for MR, including imaging in the presence of cadaveric synovial fluid and the addition of saline and gadolinium-DTPA (Gd-DTPA).

Received November 26, 1986; accepted after revision February 5, 1987.

P. C. Hajek is the recipient of the Erwin Schroedinger Stipendium fellowship award J0062, Austria.

This work was supported in part by Veterans Administration grant SA306.

[1] All authors: Departments of Radiology, University of California Medical Center, San Diego, and Veterans Administration Medical Center, 3350 La Jolla Village Dr., San Diego, CA 92161. Address reprint requests to D. Resnick at VA Medical Center.

AJR 148:1153–1157, June 1987
0361–803X/87/1486–1153

Materials and Methods

In Vitro Analysis

Signal intensities of 0.9% saline and Gd-DTPA-dimeglumine (Magnevist Schering AG, Berlin, W. Germany) diluted with saline to a concentration of 500 μM were measured and compared by using the region-of-interest 2.0 system software package [10]. These fluids were chosen because of their preferred use as contrast agents in another investigation (Hajek PC, Baker LL, Sartoris DJ, Neumann CH, Resnick D, unpublished data). MR imaging of the respective solutions was performed with a Signa 1.5-T system (General Electric) and a standard head coil. Spin-echo pulse techniques were used with repetition times (TR) of 600 and 2000 msec and echo times (TE) of 25 msec, and 20 and 70 msec, respectively. A 128 × 256 data-acquisition matrix and one signal average were used. Signal intensities of fresh cadaveric articular cartilage were measured and compared with saline and Gd-DTPA by using system software [10].

Cartilage Lesion Analysis

Six fresh cadaveric knees with intact articular cartilage on the femoral condyles (no degenerative erosive changes on gross pathologic examination) were studied. Each joint was surgically opened, and five circular, full-thickness (2-mm depth) cartilage lesions were created in either the medial or the lateral femoral condyle by using precision hand drills. Defects ranged from 1 to 5 mm in diameter (Fig. 1). Care was taken not to extend lesions beyond the cartilage layer into bone or bone marrow. The joint space and soft tissue of the knees were then surgically closed in two layers by using interrupted sutures. Knees were imaged with a variety of imaging sequences and parameters under three conditions: without intraarticular contrast material, with intraarticular saline, and with intraarticular Gd-DTPA.

Imaging was performed on a 1.5-T GE Signa scanner (General Electric Medical Systems) with a prototype round 12.7-cm-diameter surface coil positioned laterally adjacent to the femoral condyle of interest. Spin-echo pulsing sequences (TR/TE) were used for T1-weighted single-echo images (600/25 msec) and T2-weighted multi-echo images (2000/20, 2000/70 msec). The field of view used routinely was 16 cm with contiguous slice thicknesses of 3–5 mm. Additional images were acquired with sections 3-mm thick (1.5-mm intervals) and 5-mm thick (1-mm intervals). Images were obtained in the sagittal plane with an acquisition matrix of either 128 × 256 or 256 × 256, resulting in pixel sizes of 1.25 × 0.625 mm or 0.625 × 0.625 mm, respectively. Either one or two excitations were used. The imaging time per sequence was 1.5–34 min. Images were reviewed and compared to establish the size of the smallest detectable cartilage lesion for each combination of imaging techniques and intraarticular fluids. Presence or absence of visualization of different-sized lesions was used in the determination of accuracy. Measurement of lesion diameter was not used because of inherent inconsistencies related to pixel size, partial-volume effect, field inhomogeneity, and other system specifications.

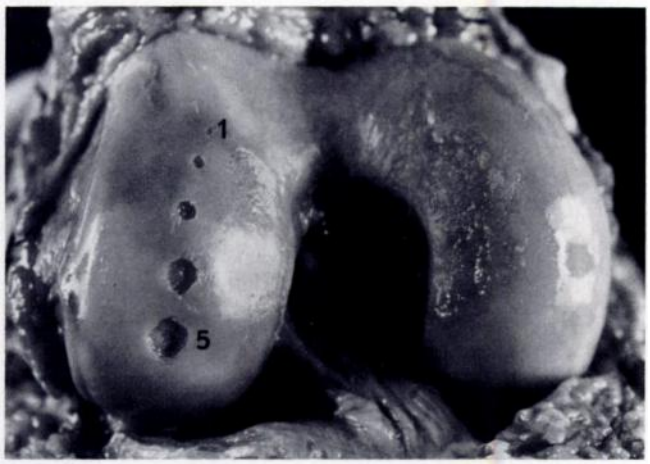

Fig. 1.—Fresh cadaver knee with artificially created cartilage defects 1–5 mm in diameter. Note incidental degenerative alterations in articular cartilage of opposite condyle.

Results

In Vitro Analysis

Signal-intensity data were expressed as a percentage indicating contrast present in the image (0% signifying absent signal, as for cortical bone; 100% signifying maximum signal intensity). For the TR 600/TE 25 sequence, signal-intensity difference for saline vs articular cartilage was 7.2%; for 500 μM Gd-DTPA, 62%. For the TR 2000/TE 20 sequence, signal-intensity difference for saline vs cartilage was 5%; for 500 μM Gd-DTPA, 60%. For the TR 2000/TE 70 sequence, signal-intensity difference for saline vs cartilage was 20%; for Gd-DTPA, 65%.

Signal-intensity differences between hyaline cartilage, saline, and Gd-DTPA were assessed to determine if there was sufficient contrast for cartilage defect visualization. In general, signal-intensity differences were highest between cartilage and Gd-DTPA (60–65%) on all sequences and lowest between cartilage and saline (7%) on T1-weighted sequences. The lowest signal-intensity difference affording sufficient contrast for visualization of separate structures was between saline and cartilage at 20%.

Cartilage Lesion Analysis

Six cadaveric knees with articular cartilage lesions placed by precision hand drilling were imaged to document and compare the smallest defect seen with various imaging parameters in the presence of cadaveric synovial fluid, 0.9% saline, and 500 μM Gd-DTPA. These results are summarized in Table 1. In general, cartilage defects were not appreciated on T1-weighted (TR 600/TE 25 msec) and balanced (TR 2000/TE 20 msec) images without prior intraarticular injection of fluid (Figs. 2B and 3B) unless defects were filled by air introduced as an artifact when knee lesions were made. However, defects 3 mm or larger were consistently seen on T2-weighted (TR 2000/TE 70 msec) images owing to partial filling by air and/or existent cadaveric synovial fluid. After intraarticular injection of 0.9% (weight/volume) saline, defects greater than or equal to 3 mm in diameter were consistently and confidently identified with T2-weighted sequences. Intraarticular Gd-DTPA allowed for delineation of lesions greater than or equal to 2 mm in size on all sequences (Fig. 4). Cartilage defects appeared as discrete areas of high-signal intensity contrasted by adjacent intact articular cartilage,

which was of intermediate signal intensity. The observed pattern was consistent with filling of the induced lesions by intraarticular fluid (Figs. 2–4).

Owing to sufficient in vitro signal-intensity differences between saline and cartilage on T2-weighted sequences and between Gd-DTPA and cartilage on all sequences, cartilage lesions were seen equally well with either one (Fig. 4B) or two (Fig. 4A) excitations, contiguous or interspaced 3-mm (Fig. 3) to 5-mm (Fig. 2) slice thicknesses, and 128 × 256 (Fig. 4D) or 256 × 256 (Fig. 4C) data-acquisition matrices. The shortest imaging time required for delineation of a 3-mm cartilage defect (the smallest detectable lesion in the presence of cadaveric synovial fluid or after saline injection) was 5 min with interspaced slices (Fig. 3A). This minimum time was shortened to 1.5 min with prior intraarticular injection of Gd-DTPA and the use of interspaced slices (Fig. 4D).

Discussion

Numerous clinical applications for MR imaging have been investigated in the evaluation of articular disorders affecting the knee and other sites [5, 7, 9, 12, 13] (Hajek PC, Baker LL, Sartoris DJ, Neumann CH, Resnick D, unpublished data). The technique has proven capable of showing meniscal, ligamentous, and adjacent soft-tissue abnormalities as well as gross cartilaginous lesions and degenerative alterations involving large segments of cartilage [1, 3, 14, 15]. Since intraarticular saline and Gd-DTPA have been shown to significantly improve the delineation of subtle structural joint defects [16], MR arthrography was used to see if cartilage lesion detectability could be enhanced.

In this investigation, full-thickness cartilage defects measuring 5 mm in diameter could not be identified on either T1-weighted or balanced MR images in the presence of saline or cadaveric synovial fluid despite imaging times of up to 34 min per series with 3-mm contiguous slices, 256 × 256 data-acquisition matrices, and two excitations. This limitation is explained by the inadequate in vitro signal intensity difference (7%) found between articular cartilage and 0.9% saline, and by the results of another investigation [16] in which inadequate signal intensity differences were found on T1-weighted images between articular cartilage and solutions of human serum albumin prepared in concentrations to approximate nontraumatic, noninflammatory synovial fluid [16, 17]. On T2-weighted images of joints in which no additional fluid was injected, recognition of defects of 3–5 mm in size was sometimes possible because of partial filling by cadaveric synovial fluid. This finding is again explained by the results of the previous study [16], in which in vitro signal-intensity differences between articular cartilage and albumin solutions (prepared in concentrations similar to normal synovial fluid) increased to 31% on T2-weighted images. With intraarticular saline, cartilage defects of 3–5 mm were consistently and confidently detected (Figs. 2 and 3) because of the complete filling of the defects by an injection volume of 35 ml and sufficient (20%) in vitro signal-intensity difference between articular cartilage and saline. Confident appraisal of the quality and integrity of articular cartilage thus becomes possible only with the use of long-TR/TE imaging sequences in the presence of nonproteinaceous or low-protein concentration joint fluid.

TABLE 1: Smallest Cartilage Defects Seen in Cadaver Knees

Contrast Medium	Smallest Defect Imaged		
	Size (mm)	TR/TE (msec)	Minimum Imaging Time (min:sec)
Cadaveric synovial fluid	3	2000/70	9:24
Saline	3	2000/70	9:24
Gd-DTPA	2	600/25	
		2000/20	2:49[a]
		2000/70	

Note.—All images were obtained with contiguous 3- and 5-mm slice thicknesses, one and two signal excitations, and 128 × 256 and 256 × 256 data-acquisition matrices. TR = repetition time; TE = echo time.

[a] Decreased to 1:25 with interspaced slice thicknesses.

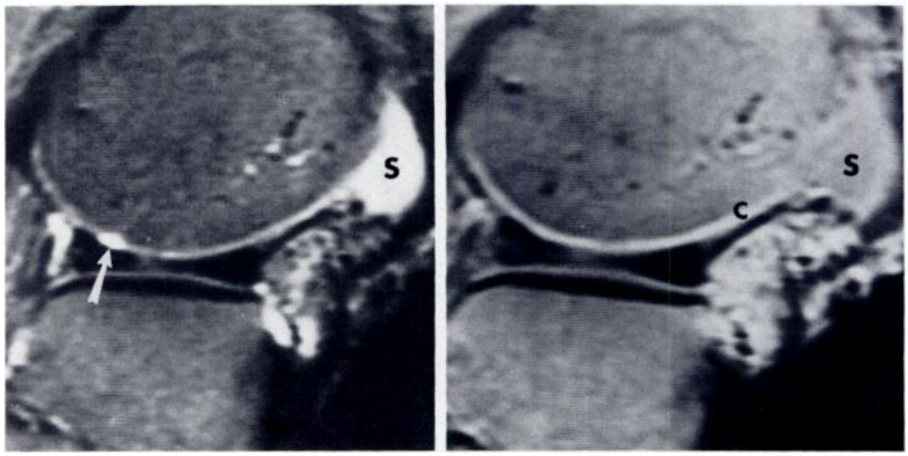

Fig. 2.—*A*, T2-weighted image (TR = 2000 msec/TE = 70 msec, 5-mm slice thickness) after intraarticular injection of 0.9% (weight/volume) saline (s) shows 3-mm cartilage defect (*arrow*).

***B*, Balanced image (TR = 2000 msec/TE = 20 msec, 5-mm slice thickness). Saline (s) and articular cartilage (c) exhibit similar signal intensities, and defect cannot be identified.**

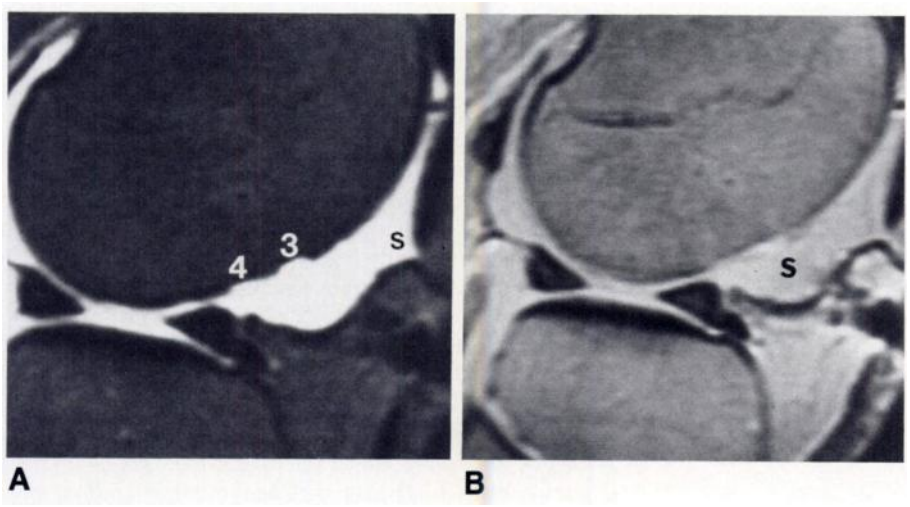

Fig. 3.—Data-acquisition matrix: 128 × 256, 3-mm contiguous slices, one signal excitation, imaging time = 9 min 24 sec. Imaging time reduces to 5 min with use of interspaced slices.

***A*, T2-weighted image (TR = 2000 msec/TE = 70 msec) after intraarticular injection of 0.9% (weight/volume) saline (s) clearly shows 3- and 4-mm cartilage defects.**

***B*, Balanced image (TR = 2000 msec/TE = 20 msec). Defects cannot be identified with certainty. s = saline.**

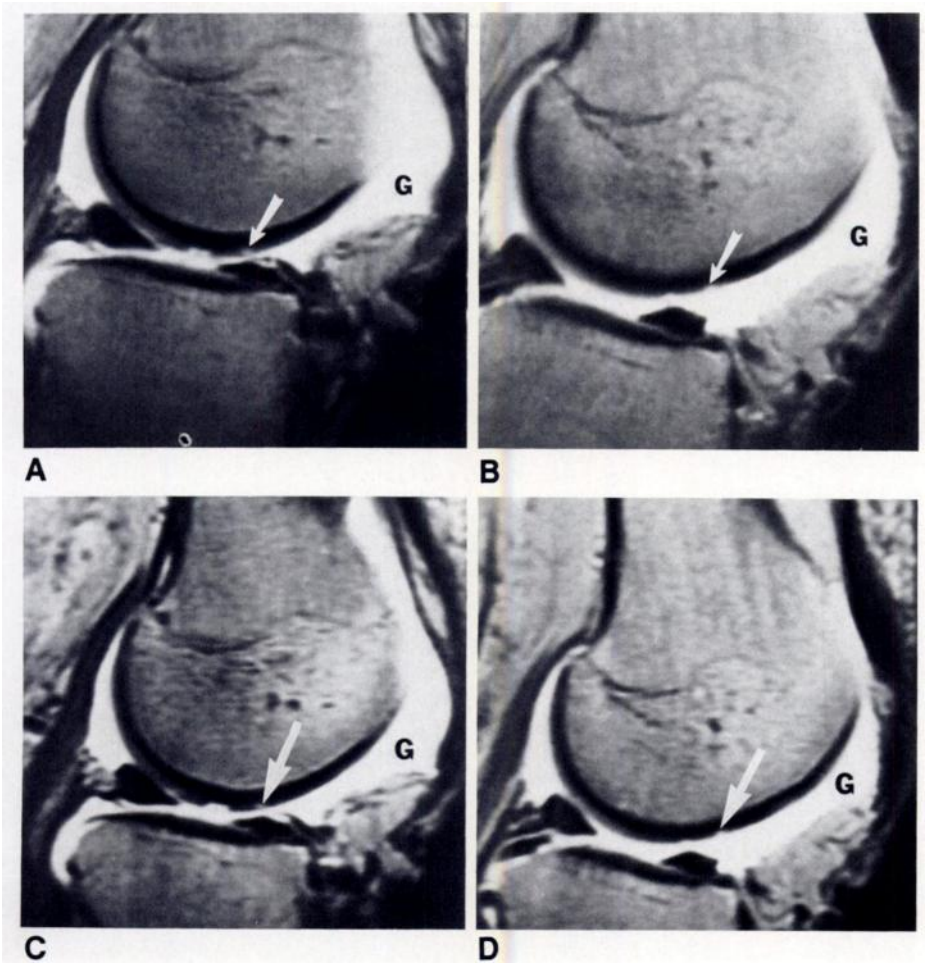

Fig. 4.—MR images (TR = 600 msec/TE = 25 msec) of cartilage defects after intraarticular administration of 500 μM Gd-DTPA (G).

***A* and *B*, 5-mm contiguous slices, 256 × 256 data-acquisition matrix. Smallest defect seen (*arrows*) is 2 mm in diameter, regardless of the number of excitations (*A*, two signal excitations, imaging time = 10 min 18 sec; *B*, one signal excitation, imaging time = 5 min 11 sec).**

***C* and *D*, 3-mm slice thicknesses with 1.5-mm interslice gap, one signal excitation. Smallest identifiable defect (*arrows*) was 2 mm in diameter, regardless of data-acquisition matrix (*C*, 256 × 256 matrix, imaging time = 2 min 41 sec; *D*, 128 × 256 matrix, imaging time = 1 min 25 sec).**

Intraarticular Gd-DTPA at a concentration of 500 μM not only improved the detectability of cartilage defects, allowing lesions as small as 2 mm in diameter to be seen, but also significantly decreased the required imaging time because of its high in vitro signal-intensity difference relative to articular cartilage on all imaging sequences. Both of these factors are important in rendering MR an accurate and cost-effective diagnostic tool. Imaging time for cartilage defects 2 mm in diameter can be as short as 1 min 25 sec.

The minimum size of osseous defects detectable by MR (such as cysts associated with osteoarthritis that would appear as marrow defects) was not assessed in this investigation. The cartilage defects created in this study may not be strictly comparable to cartilage defects in living patients since physiologic responses in adjacent tissues may well alter the detectability and size of the defects. Presence of inflammatory and posttraumatic joint effusions, for example, could potentially increase the sensitivity of MR in detecting cartilage lesions because of their increased protein and methemoglobin concentrations, respectively, by increasing signal-intensity differences to enhance articular cartilage visualization [16, 18].

Relevant clinical situations in which MR imaging could be useful in detecting articular cartilage defects would be those involving partial or complete loss of cartilage. Specifically, these would include chondral fractures, osteochondritis dissecans, osteoarthritis, crystal-induced arthropathy, and spontaneous osteonecrosis [19], as well as acute peripheral joint trauma in which cartilage defects accompany other intra- or extraarticular injuries.

This investigation did not compare the relative merits of MR imaging and arthrography combined with tomography or arthroscopy—the methods most widely used for imaging chondral and osteochondral defects [6, 11, 20]. Conceivably, MR imaging could provide an alternative method in cases of pure chondral injury where no bone accompanies the cartilage fragments.

As the use of MR imaging increases in the diagnosis of joint injuries, it becomes increasingly important for the radiologist to be aware of the limitations and capabilities of MR in evaluating articular cartilage. In summary, this investigation has shown that discrete cartilage lesions as small as 3 mm in diameter can be seen with T2-weighted sequences, regardless of other imaging parameters such as number of signal averages, size of acquisition matrix, and slice thickness. Diagnostic capabilities increase, however, after intraarticular injection of Gd-DTPA in a 500-μM concentration. Of potentially greater practical importance, required time for imaging cartilage defects decreases dramatically with intraarticular Gd-DTPA, permitting acquisition of diagnostic series with total scanning times of less than 1.5 min.

REFERENCES

1. Burk DL, Kanal E, Brunberg JA, Johnstone GF, Swensen HE, Wolf GL. 1.5-T surface-coil MRI of the knee. *AJR* **1986**;147:293–300
2. Reicher MA, Rauschning W, Gold RH, Bassett LW, Lufkin RB, Glenn W. High-resolution MRI of the knee joint: normal anatomy. *AJR* **1985**; 145:895–902
3. Reicher MA, Bassett LW, Gold RH. High-resolution magnetic resonance of the knee joint: pathologic correlation. *AJR* **1985**;145:903–909
4. Turner DA, Prodromos CC, Petasnick JP, Clark JW. Acute injury of the ligaments of the knee: magnetic resonance evaluation. *Radiology* **1985**;154:717–722
5. Reicher MA, Hartzman S, Duckwiler GR, Bassett LW, Anderson LJ, Gold RH. Meniscal injuries: detection using MR imaging. *Radiology* **1986**;159:753–758
6. Sartoris DJ, Kursunoglu S, Pineda C, et al. Detection of intra-articular osteochondral bodies in the knee using computed arthrotomography. *Radiology* **1985**;155:447–450
7. Ghelman B. Meniscal tears of the knee: evaluation by high-resolution CT combined with arthrography. *Radiology* **1985**;157:23–27
8. Johnson LL. *Diagnostic and surgical arthroscopy*. St. Louis: Mosby, **1981**
9. Koenig H, Lucas D, Meissner R. The wrist: a preliminary report of high-resolution MR imaging. *Radiology* **1986**;169:463–467
10. General Electric Medical Systems. *Operating the Signa system (0.5, 1.0 and 1.5 Tesla) OMSI*, rev. 7. Milwaukee: General Electric, **1986**
11. Wolfe RD. *Knee arthrography: a practical approach*. Saunders monographs in clinical radiology, vol. 23. Philadelphia: Saunders, **1984**
12. Li DK, Adams ME, McConkey JP. Magnetic resonance imaging of the ligaments and menisci of the knee. *Radiol Clin North Am* **1986**;24: 209–227
13. Sims RE, Genant HK. Magnetic resonance imaging of joint disease. *Radiol Clin North Am* **1986**;24:179–188
14. Passariello R, Masciocchi C, DePaulis F, et al. MRI versus CT for characterization of capsulo-ligamentous lesions of the knee joint. Presented at the annual meeting of the Society for Magnetic Resonance in Medicine, Montreal, Quebec, Canada, August **1986**
15. Bellon EM, Coleman PE, Keith MW, et al. MRI, arthrography and arthroscopy in evaluation of internal derangements of the knee: a prospective correlative study. Presented at the annual meeting of the Society for Magnetic Resonance in Medicine, Montreal, Quebec, Canada, August **1986**
16. Hajek PC, Sartoris DJ, Resnick D. Potential contrast agents for MR-arthrography: in vitro evaluation and practical observations. *AJR* (in press)
17. McCarty DJ. Synovial fluid. In: McCarty DJ, ed. *Arthritis and allied conditions*. Philadelphia: Lea & Febiger, **1985**:54–75
18. Beltran J, Noto AM, Herman LJ, Mosure JC, Burk JM, Christoforidis AJ. Joint effusions: MR imaging. *Radiology* **1986**;158:133–137
19. Resnick D, Niwayama G. Physical injury. In: Resnick D, Niwayama G, eds. *Diagnosis of bone and joint disorders with emphasis on articular abnormalities*. Philadelphia: Saunders, **1981**:2258–2272
20. Gilley JS, Gelman MI, Edson M, et al. Chondral fractures of the knee: arthrographic, arthroscopic, and clinical manifestations. *Radiology* **1981**;138:51–54